


Surface modification nanoporous titanium oxide films using continuous wave CO₂ laser

Wen-Tse Hsiao¹  · Chih-Chung Yang¹ · Shih-Feng Tseng¹ · Donyau Chiang¹ · Kuo-Cheng Huang¹ · Keh-Moh Lin² · Ming-Fei Chen³

Received: 16 October 2015 / Accepted: 28 February 2016 / Published online: 14 March 2016
© Springer-Verlag Berlin Heidelberg 2016

Abstract This study investigated the characteristics of titanium dioxide (TiO₂) films modified through laser annealing by using a CO₂ laser source (CSS 500 AIR, Spectral Inc., Italy) with a wavelength of 10,600 nm and a continuous wave mode. Commercial TiO₂ thin films with a thickness of 100 nm were prepared through radio-frequency magnetron sputtering on soda-lime glass substrates. The optical properties (optical absorption and transmittance spectra), surface morphology, and surface chemical composition characteristics of the TiO₂ films depended on the laser irradiation conditions. The characteristics of the films were systematically analyzed using a ultraviolet–visible near-infrared spectrophotometer, an X-ray photoelectron spectroscopy, and a field emission scanning electron microscope. The experimental results demonstrated that the experimental transmittance spectra exhibited slight changes caused by laser annealing and a maximum transmittance in the visible region of approximately 91.4 %. The absorbance of all annealed TiO₂ films exceeded that of as-deposited films. Moreover, the absorption band edge moved toward the long-wavelength side (red shift) as the annealing speed decreased because the heat applied during annealing caused the TiO₂ film grains to grow. Diffusion

and mobility between the films and glass substrates during laser annealing segregated elemental Ag.

1 Introduction

Titanium dioxide (TiO₂) has three crystal forms (anatase, brookite, and rutile). Because crystalline TiO₂ exhibits superior chemical stability, a high-energy band gap, and a high dielectric constant, it is commonly used in a wide range of applications, including photocatalysts [1], solar cells [2], and oxide sensors [3]. The use of fossil energy, with the resulting discharge of exhaust gases, has become the primary cause of the greenhouse effect, leading to dangerous environmental consequences. Owing to the demand for alternative energy and increased environmental awareness in past years, many nations are actively seeking to use renewable energy resources such as photovoltaic solar energy, wind energy, potential energy, and biomass energy. Of these, photovoltaic solar energy is one of the most efficient. It is generated using silicon-based thin-film solar cells. Nanoscale TiO₂ films are used as working electrodes for dye-sensitized solar cells (DSSCs) because they are highly efficient. A DSSC is a promising device for generating useful power from solar energy because it has a lower production cost than that of conventional semiconductor solar cells and high light conversion efficiency [2, 4, 5]. However, the surface morphology of the working electrode can considerably affect cell efficiency. Therefore, several studies have investigated the surface modification of TiO₂ electrodes for DSSCs. Various methods of surface modification by using a laser source and rapid thermal annealing (RTA) have been proposed. Laser annealing is more effective than thermal annealing because it produces higher energy in a localized area over a shorter period.

✉ Wen-Tse Hsiao
wentse@itrc.narl.org.tw

¹ Instrument Technology Research Center, National Applied Research Laboratories, No. 20, R&D Rd. VI, Hsinchu Science Park, Hsinchu 30076, Taiwan

² Department of Mechanical Engineering, Southern Taiwan University of Science and Technology, Tainan, Taiwan

³ Department of Mechatronics Engineering, National Changhua University of Education, Changhua, Taiwan

Numerous studies have reported the use of laser treatment technology to modify TiO₂ photoanodes for DSSCs. Various laser annealing processes based on the excimer laser, neodymium-doped yttrium aluminum garnet laser, and ultraviolet (UV) sources have been proposed for annealing thin films [6]. Pan et al. [7] reported a rapid and low-temperature process for fabricating composite TiO₂ electrodes for DSSCs on glass and plastic substrates by using a homogenized KrF excimer laser source with a wavelength of 248 nm. Kim et al. [8] proposed the laser-induced forward transfer of nanocrystalline TiO₂ films onto a fluorine-doped SnO₂-coated glass substrate by using a pulse UV laser. Moreover, they developed mesoporous TiO₂ photoelectrodes from a colloidal solution of nanopowders by using a quasi-continuous-wave UV laser [9]. Overschelde et al. [10] used a KrF excimer laser to increase the laser fluence from 0.05 to 0.40 mJ/cm². Experimental results indicated that the as-deposited films were amorphous, whereas the irradiated films had an anatase structure. The crystalline structure of the films varied substantially as a function of fluence up to 0.125 J/cm². The irradiated areas exhibited a considerably modified microstructure with nanoscale features. Pu et al. [11, 12] used a KrF excimer laser to irradiate nanoporous TiO₂ films for DSSC applications. Laser irradiation changed the structure of the TiO₂ films from anatase to rutile. The amount of the transformed phase depended on the power density of the laser. Cha et al. [13] developed an ultrafast and low-temperature laser annealing process for patterning crystalline TiO₂ nanostructures. They used a high-power infrared (IR) laser [wavelength of 1064 nm and continuous wave (CW) mode] and galvanometric scanner for annealing. The TiO₂ patterns were annealed using a laser at powers of 30, 50, 70, and 100 W for annealing times of 30–180 s. Raman spectra revealed TiO₂ patterns on the glass substrates. Moreover, a higher laser power formed larger grains, as determined from the highest peak in the Raman spectrum. Chung et al. [14] used the sol-gel process to spin-coat TiO₂ films on Si (100) wafers and annealed the films by using a CO₂ laser at 1.5 W. Wang et al. [15] used the sol-gel dip-coating method for the thermal annealing of crystalline TiO₂ films at temperatures higher than 400 °C. The optical properties of the films depended on thermal processing. Experimental results demonstrated that the refractive index increased with an increasing thermal annealing temperature. The refractive index values ranged from 1.98 to 2.57 at a He-Ne laser wavelength of 633 nm.

The current study investigated the characteristics of TiO₂ films modified through laser annealing by using a CO₂ laser source (CSS 500 AIR, Spectral Inc., Italy) with a wavelength of 10,600 nm, a CW mode, a moving stage, and varying parameters. The characteristics of the films were systemically analyzed using a UV-visible near-IR

(UV-Vis/NIR) spectrophotometer, a field emission scanning electron microscope (FE-SEM), and an X-ray photoelectron spectroscopy (XPS).

2 Experiment

2.1 Preparation of TiO₂ thin films and laser annealing system

Commercial TiO₂ films with a thickness of 100 nm were prepared through radio-frequency magnetron sputtering on soda-lime glass substrates at room temperature in an air atmosphere. To ensure that the dimensions of all samples were the same, the glass substrates were diced to dimensions of 30 mm² by using a diamond wheel machine, and the machined specimens were cleaned in an ultrasonic cleaner by using 75 vol% alcohol solution and 25 vol% distilled water. The specimens were dried on a spin coater and subsequently baked and cured at 50 °C for 5 min. Table 1 summarizes the properties of the as-deposited TiO₂ films on glass substrates.

The CO₂ laser annealing system comprised a laser source, beam collimation optics, and a dual-axis moving stage. The CO₂ laser source had a wavelength of 10,600 nm and a maximum average power of 40 W. The specimens were irradiated with a laser beam, which was delivered by the optical system including the mirrors and collimation optics. Table 2 lists the complete specifications of the CO₂ laser annealing system.

2.2 Characterization

The surface topographies, surface morphologies, and cross-sectional views of the as-deposited TiO₂ films on glass substrates were recorded using an FE-SEM (JEOL JSM-

Table 1 Properties of TiO₂ films deposited on soda-lime glass substrates used in experiments

Substrate	TiO ₂ films thickness (nm)	Average optical transmission (%) (at wavelength of 400–800 nm)
Soda-lime glass (1.1 mm)	100	~ 80 %

Table 2 Specification of the CO₂ laser annealing system

Parameters	Values
Wavelength (nm)	10,600
Maximum power (W)	~ 40
Spatial mode	Near TEM ₀₀
Operation mode	Continuous wave

Fig. 1 SEM morphology of the as-deposited TiO₂ films. **a** Top view and **b** cross-sectional view

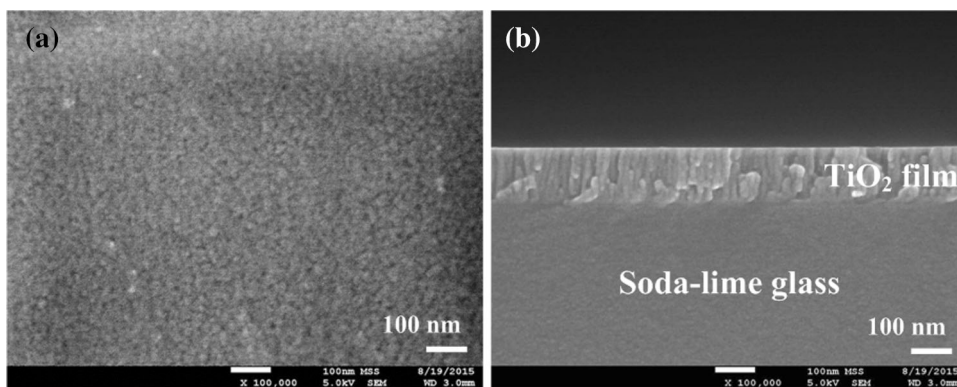
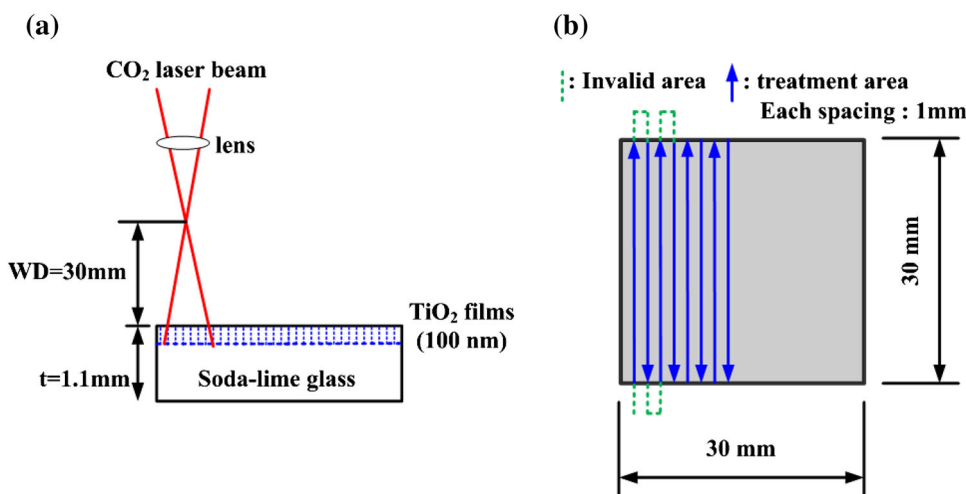


Fig. 2 **a** Schematic diagram of the experimental setup and **b** schematic diagram of the laser annealing process on TiO₂ films



7500f). The optical transmittance and reflectance were measured using a UV–Vis/NIR spectrophotometer (Jasco V-670). The chemical compositions were determined using a high-resolution XPS (ULVAC-PHI Quantera II, Japan). Figure 1 shows the top view and cross-sectional SEM morphologies of the TiO₂ films deposited on soda-lime glass substrates.

2.3 Experimental procedure

Figure 2 schematically depicts the laser annealing process applied to the TiO₂ films. The specimen dimensions were 30 mm × 30 mm × 1.1 mm. The TiO₂ films were annealed using a working distance of 30 mm and an annealing laser beam diameter of 2 mm. The annealing area was 45 mm², covering the entire specimen.

The laser annealing system was used to anneal the TiO₂ films. The annealing parameters were adjusted as follows. To obtain favorable annealing results (to prevent microcracks and damage to the substrate), the laser power was set to 30 W. The speed of the dual-axis moving stage was set to 15, 20, 25, or 30 mm/s. Each annealing beam pitch had

Table 3 Processing parameter values of laser annealing TiO₂ films

Laser power (W)	Each spacing (mm)	Annealing speed (mm/s)
40	1	15
		20
		25
		30

an equal spacing of 1 mm to yield favorable annealing quality. Table 3 lists the laser annealing parameters for the nanoporous TiO₂ films annealed using the CO₂ laser.

3 Results and discussion

3.1 Optical properties of the as-deposited and annealed TiO₂ films

The laser annealing parameters, including laser power and annealing speed, affected the properties of the treated films [16–18]. Figure 3 shows the transmittance spectra of TiO₂

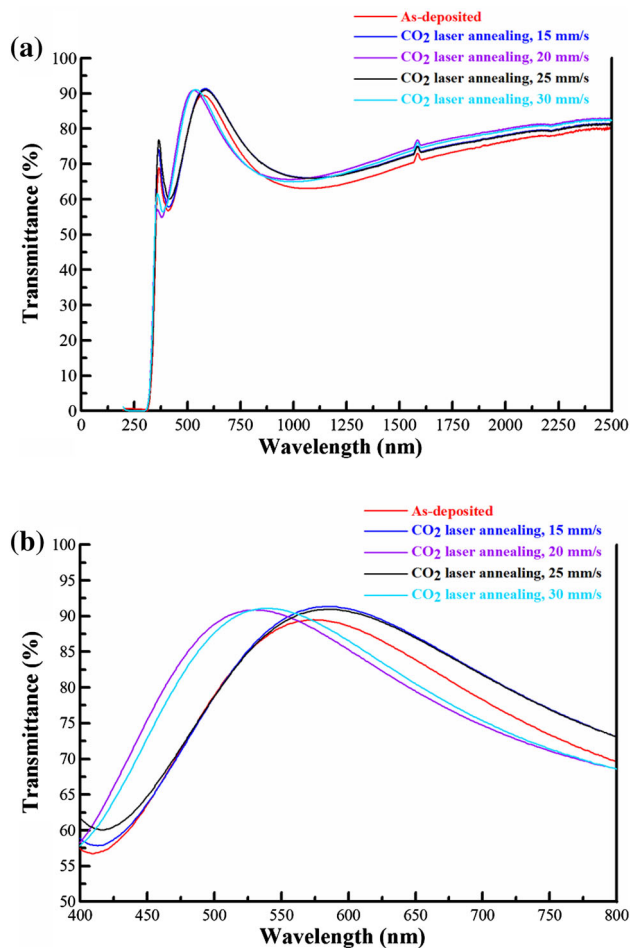


Fig. 3 Transmittance spectra of as-deposited and annealed TiO₂ films in different wavebands. **a** 300–2500 nm and **b** 400–800 nm

films that were annealed under various conditions at wavelengths of 300–2500 and 400–800 nm. Figure 3 indicates that the maximum transmittance of the as-deposited TiO₂ films was 89.68 %. The laser power fixed at 30 W, and the TiO₂ films were annealed at various speeds of 15, 20, 25, and 30 mm/s; the measurements demonstrated that the transmittance decreased as the annealing speed increased. The maximum transmittance values of all annealed TiO₂ films exceeded those of the as-deposited films. When the annealing speed was 15 mm/s, a maximum transmittance of 91.35 % was obtained. A lower annealing speed caused heat to accumulate on the TiO₂ films; therefore, the transmittance of the annealed TiO₂ films increased, as reported by several studies. Sankar and Gopchandran [19] reported that the transmittance values of deposited and annealed TiO₂ films increased with increasing annealing temperature. Yoo et al. [20] observed that the transmittance of samples annealed through RTA increased with increasing annealing temperature. Bedikyan et al. [21] reported that the optical properties of films were

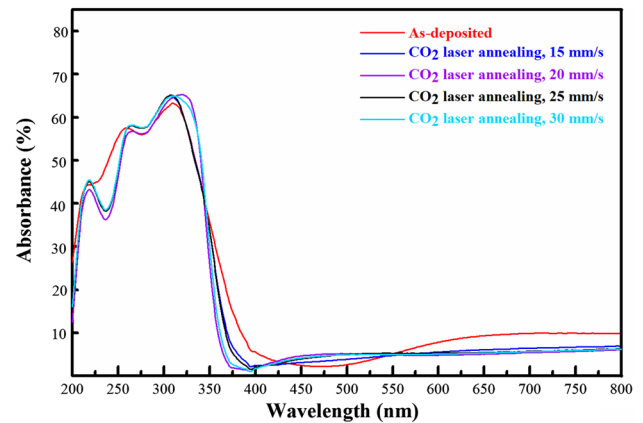


Fig. 4 Optical absorbance of as-deposited and annealed TiO₂ films was ranging from ultraviolet to visible spectrum

dependent on the substrate and annealing temperature. According to the UV–Vis spectra, the transmittance increased with increasing annealing temperature.

Figure 4 shows the absorbance spectra of TiO₂ films annealed under various conditions at wavelengths from UV to visible. A comparison of the as-deposited and annealed specimens revealed that the annealed TiO₂ films absorbed considerably more of the UV spectrum than they did of the visible spectrum. Furthermore, the absorbance values of all annealed TiO₂ films exceeded those of the as-deposited films. The absorption band edge moved toward the long-wavelength side (red shift) as the annealing speed decreased, because heating during annealing causes the grains in the TiO₂ film to grow. This movement of the absorption band during annealing of TiO₂ films has also been observed by Hanini et al. [22] and Khan et al. [23].

3.2 XPS analysis of the as-deposited and laser-annealed TiO₂ films

The compositions of the as-deposited TiO₂ films were determined using the high-resolution XPS, and the corresponding survey spectra are shown in Fig. 5a. The spectra indicated that the TiO₂ films contained the elements Ti, O, C, and Na. Barrie and Street [24] reported binding energies of 1071.8 and 1072.5 eV for the Na metal in Na₂O. Figure 5b–d depicts the XPS scan spectra of the as-deposited TiO₂ films for Ti 2p, O 1s, and C 1s, respectively.

Figure 5b shows the Ti 2p core spectra; two photoemission peaks centered at 457.77 and 463.57 eV are assigned to Ti 2p_{3/2} and Ti 2p_{1/2}, respectively. The spectrum is consistent with that of standard single-crystal TiO₂ films, revealing that the TiO₂ film contained valence bonds between Ti and O atoms that were consistent with TiO₂. Calculations revealed that the full width at half maximum (FWHM) of the Ti 2p_{3/2} peak, 1.38 eV, is greater than that of the Ti 2p_{3/2} peak of standard single-crystal TiO₂ films, 1.1 eV, implying

Fig. 5 X-ray photoelectron spectroscopy (XPS) spectra for the surface of as-deposited TiO₂ films. **a** Survey spectrum, **b** Ti 2p scan, **c** O 1s scan, and **d** C 1s scan

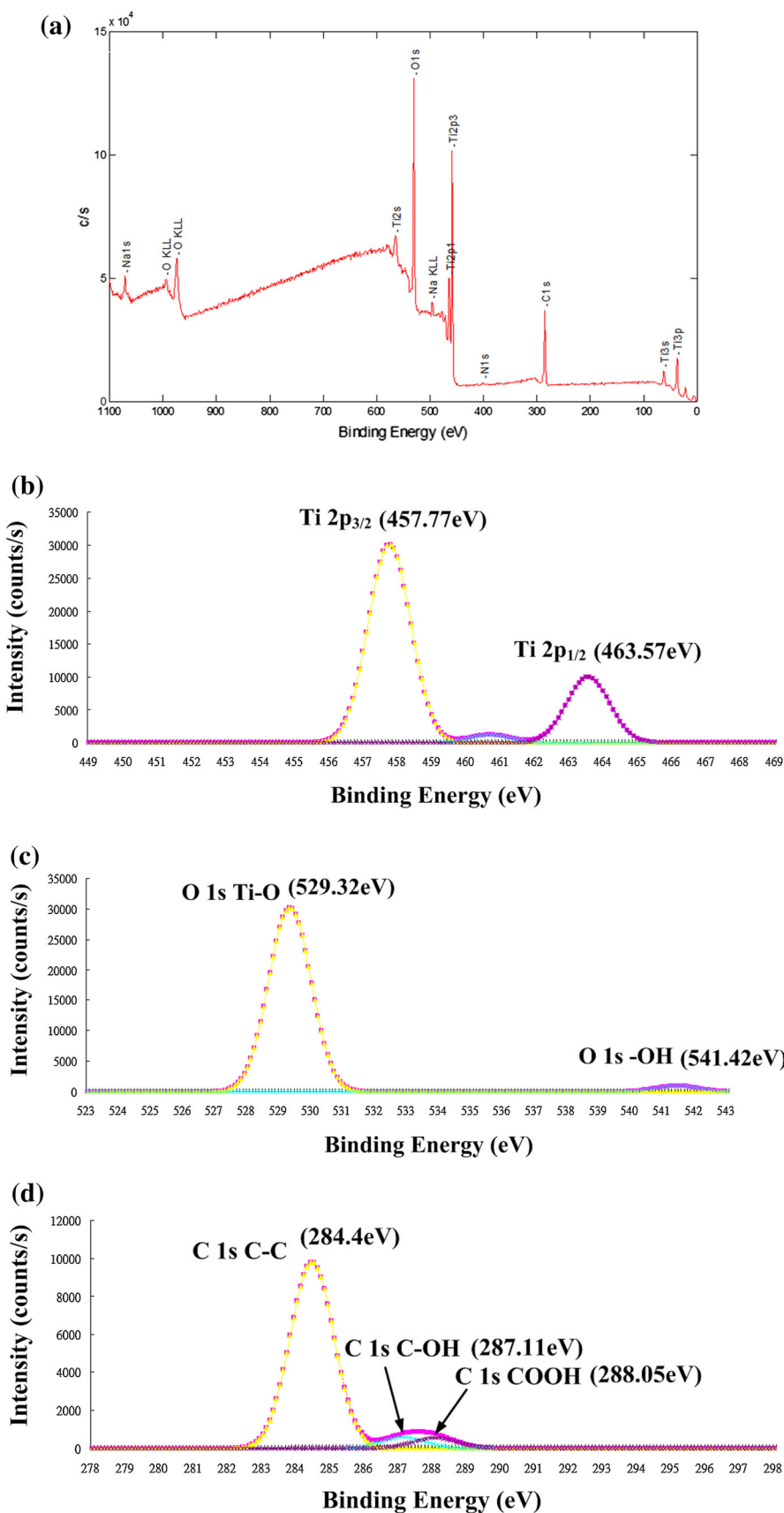


Fig. 6 X-ray photoelectron spectroscopy (XPS) spectra for the surface of annealed TiO₂ films (annealing parameters of laser power 30 W and annealing speed 15 mm/s). **a** Survey spectrum, **b** Ti 2p scan, **c** O 1s scan, and **d** C 1s scan

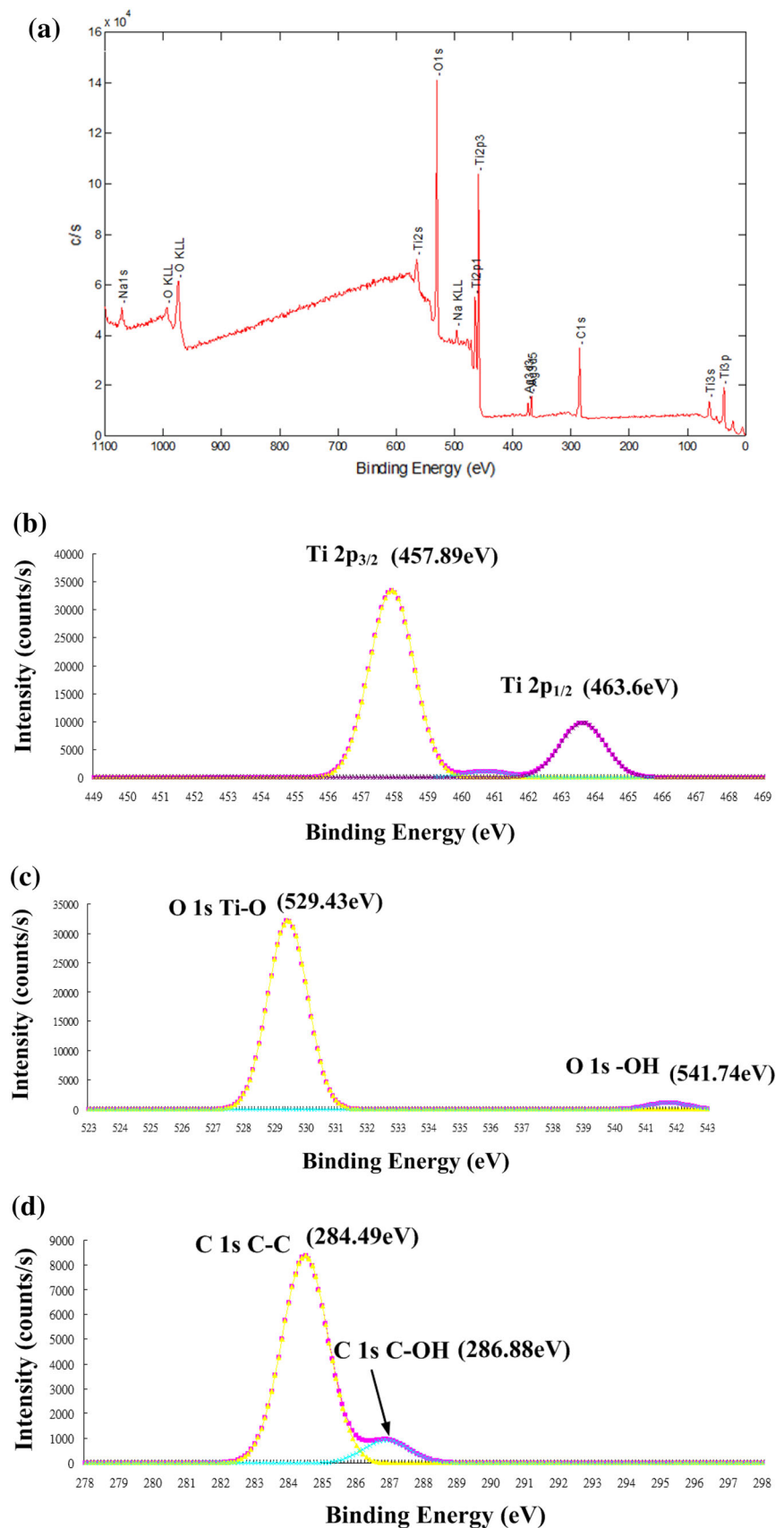
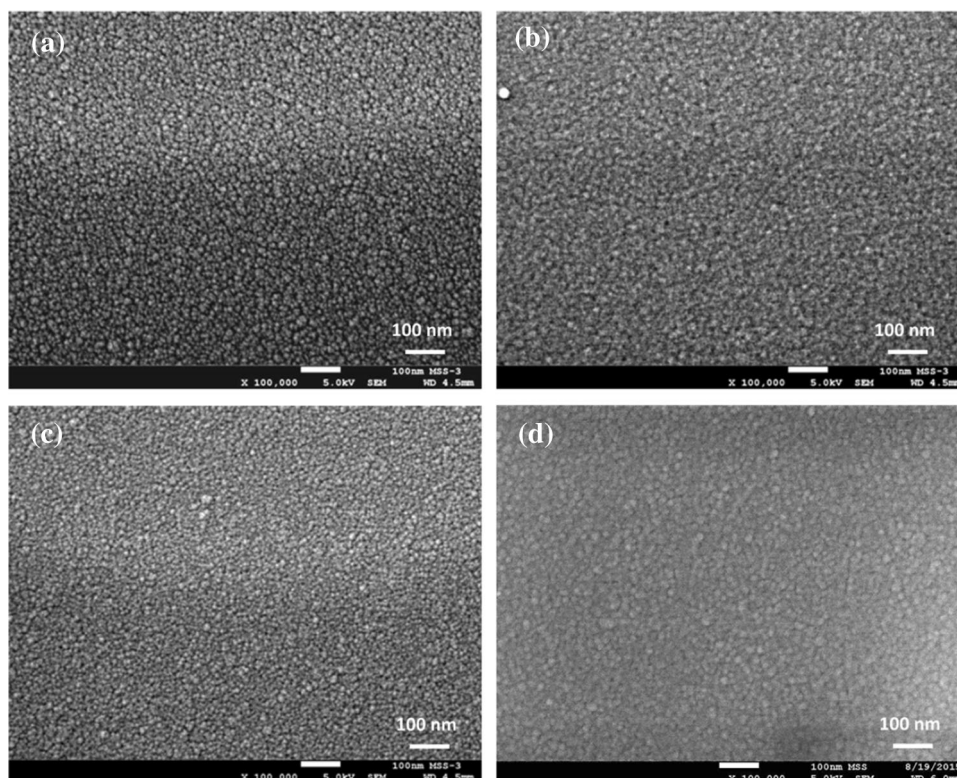


Fig. 7 SEM photography of laser annealing TiO₂ films at laser power was 30 W for different annealing speeds. **a** 15 mm/s, **b** 20 mm/s, **c** 25 mm/s, **d** 30 mm/s



that the TiO₂ films examined here are amorphous. This behavior was also reported by Liu et al. [25].

The O 1 s core-level spectra are shown in Fig. 5c; the first component is localized at 529.32 eV and is assigned to the Ti–O bond in TiO₂ [26, 29]. The second component centered at 541.42 eV corresponds to the binding energy of a hydroxyl group –OH [27]. The XPS spectrum of the as-deposited TiO₂ films shown in Fig. 5d reveals the presence of C, which was a surface contaminant on the sample. The main peak of C 1 s at 284.4 eV arises from the C–C bond, and the spectral peaks at 287.11 and 288.05 eV correspond to the C–OH and COOH bonds, respectively.

Figure 6 shows the XPS spectra of the surface of annealed TiO₂ films for a laser power of 30 W and annealing speed of 15 mm/s. Figure 6a shows the survey spectra, which demonstrate that the surfaces of the films contained Ti, O, C, Na, and Ag. Diffusion and mobility between the TiO₂ films and the soda-lime glass substrates during laser annealing caused segregation of elemental Ag.

The spectrum in Fig. 6b shows Ti 2p_{3/2} and Ti 2p_{1/2} peaks at 457.89 and 463.6 eV, respectively. All measured peaks slightly shifted relative to those of the standard single-crystal TiO₂ films, indicating that the annealed TiO₂ films contained TiO_x. Moreover, the FWHM of the Ti 2p_{3/2} peak of the annealed TiO₂ films was 1.1 eV, approximating the FWHM of the Ti 2p_{3/2} peak of standard single-crystal TiO₂ films, thus verifying that the laser-annealed TiO₂ films were indeed crystalline. Figure 6c shows the O 1 s peak at 529.43 eV,

which is associated with the bond between Ti and O. The peak at 541.74 eV corresponds to the binding energy of –OH. Therefore, the surfaces of the as-deposited TiO₂ films exhibited hydrophilic properties. The XPS spectra of the TiO₂ films in Fig. 6d reveal the presence of C, which was introduced as a surface contaminant on the sample. The C 1 s peak at 284.49 eV is associated with the C–C bond, and the spectral peak at 286.88 eV corresponds to the C–OH bond. The binding energy of the C 1 s peak is similar to that reported by Senthilkumar et al. [28].

3.3 Surface morphology and structural analysis

Figure 7 shows the surface morphologies of TiO₂ films that were annealed at powers and speeds of (a) 30 W and 15 mm/s, (b) 30 W and 20 mm/s, (c) 30 W and 25 mm/s, and (d) 30 W and 30 mm/s. The surface morphologies exhibited slight growth upon laser annealing using various laser parameters, relative to the grains of as-deposited TiO₂ films (Fig. 1a); crystalline grains were clearly observed on the surfaces of the films.

4 Conclusions

In this study, TiO₂ films were laser annealed by irradiating them with a CW-mode CO₂ laser beam. Laser annealing slightly changed the transmittance spectra, yielding a

maximum transmittance of approximately 91.4 % in the visible region. The absorbance values of all annealed TiO₂ films exceeded those of the as-deposited films in the UV spectrum. The absorption band edge moved toward the long-wavelength side (red shift) as the annealing speed decreased because heating during annealing causes growth of the grains in the TiO₂ film. Diffusion and mobility between the films and glass substrates during laser annealing caused segregation of Ag.

Acknowledgments The authors thank the Ministry of Science and Technology of Taiwan for financially supporting this research under Contract Nos. MOST 104-2221-E-492-039 and MOST 104-2622-E-492-008-CC3. Measuring supports from Ms. Nien-Nan Chu of Instrument Technology Research Center.

References

1. A. Fujishima, K. Honda, *Nature* **238**, 37 (1972)
2. B. O'Regan, M. Grätzel, *Nature* **353**, 737 (1991)
3. N. Golego, S.A. Studenikin, M. Cocivera, *J. Electrochem. Soc.* **147**, 1592 (2000)
4. M. Gratzel, *Inorg. Chem.* **44**, 6841 (2005)
5. M. Gratzel, *Electrochemistry* **79**, 760 (2011)
6. K.W. Kim, S.S. Kim, S.Y. Lee, *Curr. Appl. Phys.* **12**, 585 (2012)
7. H. Pan, S.H. Ko, N. Misra, C.P. Grigoropoulos, *Appl. Phys. Lett.* **94**, 071117 (2009)
8. H. Kim, G.P. Kushto, C.B. Arnold, Z.H. Kafafi, A. Pique, *Appl. Phys. Lett.* **85**, 464 (2004)
9. H. Kim, R.C.Y. Auyeung, M. Ollinger, G.P. Kushto, Z.H. Kafafi, A. Piqué, *Appl. Phys. A Mater. Sci. Proc.* **83**, 73–76 (2006)
10. O.V. Overschelde, R. Snyders, M. Wautelet, *Appl. Surf. Sci.* **254**, 971 (2007)
11. M.Y. Pu, J.Z. Chen, I.C. Cheng, *Int. Ceram. J.* **39**, 6183 (2013)
12. M.Y. Pu, J.Z. Chen, *Mater. Lett.* **66**, 162 (2012)
13. S. Cha, S. Lee, J.E. Jang, A. Jang, J.P. Hong, J. Lee, J.I. Sohn, D.J. Kang, J.M. Kim, *Appl. Phys. Lett.* **103**, 053114 (2013)
14. C.K. Chung, K.P. Chuang, S.Y. Cheng, S.L. Lin, K.Y. Hsie, *J. Alloys Compd.* **574**, 83 (2013)
15. X. Wang, G. Wu, B. Zhou, J. Shen, *Materials* **6**, 2819 (2013)
16. D. Wan, B. Wang, Y. Wang, H. Sun, R. Zhang, L. Wei, *J. Cryst. Growth* **253**, 230 (2003)
17. G. Gonçalves, E. Elangovan, P. Barquinha, L. Pereira, R. Martins, E. Fortunato, *Thin Solid Films* **515**, 8562 (2007)
18. H.J. Cho, S.U. Lee, B. Hong, Y.D. Shin, J.Y. Ju, H.D. Kim, M. Park, W.S. Choi, *Thin Solid Films* **518**, 2941 (2010)
19. S. Sankar, K.G. Gopchandran, *Indian J. Pure Appl. Phys.* **46**, 791 (2008)
20. D. Yoo, I. Kim, S. Kim, C.H. Hahn, C. Lee, S. Cho, *Appl. Surf. Sci.* **253**, 3888 (2007)
21. L. Bedikyan, S. Zakhariyev, M. Zakhariyeva, *J. Chem. Technol. Metall.* **48**, 555 (2013)
22. F. Hanini, A. Bouabellou, Y. Bouachiba, F. Kermiche, A. Taabouche, M. Hemissi, D. Lakhdari, *IOSR J. Eng.* **3**, 21 (2013)
23. A.F. Khan, M. Mehmood, S.K. Durrani, M.L. Ali, N.A. Rahim, *Mater. Sci. Semicond. Process.* **29**, 161 (2015)
24. A. Barrie, F.J. Street, *J. Electron Spectrosc. Relat. Phenom.* **7**, 1 (1975)
25. J. Liu, D. Yang, J. Xu, *Chin. J. Mater. Res.* **15**, 445 (2001)
26. J. Domaradzki, D. Kaczmarek, E.L. Prociow, A. Borkowska, D. Schmeisser, G. Beuckert, *Thin Solid Films* **513**, 269 (2006)
27. P.M. Kumar, S. Badrinarayanan, M. Sastry, *Thin Solid Films* **358**, 122 (2000)
28. V. Senthilkumar, M. Jayachandran, C. Sanjeeviraja, *Thin Solid Films* **519**, 991 (2010)
29. E. Aubry, J. Lambert, V. Demange, A. Billard, *Surf. Coat. Technol.* **206**, 4999 (2012)